



**HAL**  
open science

# Neural networks-based backward scheme for fully nonlinear PDEs

Huyen Pham, Xavier Warin, Maximilien Germain

► **To cite this version:**

Huyen Pham, Xavier Warin, Maximilien Germain. Neural networks-based backward scheme for fully nonlinear PDEs. 2020. hal-02196165v2

**HAL Id: hal-02196165**

**<https://hal.science/hal-02196165v2>**

Preprint submitted on 28 May 2020 (v2), last revised 10 Dec 2020 (v3)

**HAL** is a multi-disciplinary open access archive for the deposit and dissemination of scientific research documents, whether they are published or not. The documents may come from teaching and research institutions in France or abroad, or from public or private research centers.

L'archive ouverte pluridisciplinaire **HAL**, est destinée au dépôt et à la diffusion de documents scientifiques de niveau recherche, publiés ou non, émanant des établissements d'enseignement et de recherche français ou étrangers, des laboratoires publics ou privés.

# Neural networks-based backward scheme for fully nonlinear PDEs \*

Huyên PHAM<sup>†</sup>

Xavier WARIN<sup>‡</sup>

Maximilien GERMAIN<sup>§</sup>

May 28, 2020

## Abstract

We propose a numerical method for solving high dimensional fully nonlinear partial differential equations (PDEs). Our algorithm estimates simultaneously by backward time induction the solution and its gradient by multi-layer neural networks, while the Hessian is approximated by automatic differentiation of the gradient at previous step. This methodology extends to the fully nonlinear case the approach recently proposed in [HPW19] for semi-linear PDEs. Numerical tests illustrate the performance and accuracy of our method on several examples in high dimension with nonlinearity on the Hessian term including a linear quadratic control problem with control on the diffusion coefficient, Monge-Ampère equation and Hamilton-Jacobi-Bellman equation in portfolio optimization.

**Key words:** Neural networks, fully nonlinear PDEs in high dimension, backward scheme.

**MSC Classification:** 60H35, 65C20, 65M12.

## 1 Introduction

This paper is devoted to the resolution in high dimension of fully nonlinear parabolic partial differential equations (PDEs) of the form

$$\begin{cases} \partial_t u + f(\cdot, \cdot, u, D_x u, D_x^2 u) = 0, & \text{on } [0, T] \times \mathbb{R}^d, \\ u(T, \cdot) = g, & \text{on } \mathbb{R}^d, \end{cases} \quad (1.1)$$

with a non-linearity in the solution, its gradient  $D_x u$  and its hessian  $D_x^2 u$  via the function  $f(t, x, y, z, \gamma)$  defined on  $[0, T] \times \mathbb{R}^d \times \mathbb{R} \times \mathbb{R}^d \times \mathbb{S}^d$  (where  $\mathbb{S}^d$  is the set of symmetric  $d \times d$  matrices), and a terminal condition  $g$ .

The numerical resolution of this class of PDEs is far more difficult than the one of classical semi-linear PDEs where the nonlinear function  $f$  does not depend on  $\gamma$ . In fact, rather few methods are available to solve fully nonlinear equations even in moderate dimension.

- First based on the work of [Che+07], an effective scheme developed in [FTW11] using some regression techniques has been shown to be convergent under some ellipticity conditions later removed by [Tan13]. Due to the use of basis functions, this scheme does not permit to solve PDE in dimension greater than 5.
- A scheme based on nesting Monte Carlo has been recently proposed in [War18]. It seems to be effective in very high dimension for maturities not too long and linearities not too important.
- A numerical algorithm to solve fully nonlinear equations has been proposed by [BEJ19] based on the second order backward stochastic differential equations (2BSDE) representation of [Che+07] and global deep neural networks minimizing a terminal objective function, but no test on real fully nonlinear case is given. This extends the idea introduced in the pioneering papers [EHJ17; HE18], which were the first serious works for using machine learning methods to solve high dimensional PDEs.
- The Deep Galerkin method proposed in [SS18] based on some machine learning techniques and using some automatic differentiation of the solution seems to be effective on some cases. It has been tested in [AA+18] for example on the Merton problem.

---

\*This work is supported by FiME, Laboratoire de Finance des Marchés de l’Energie, and the ”Finance and Sustainable Development” EDF - CACIB Chair.

<sup>†</sup>LPSM, Université de Paris, CREST-ENSAE & FiME pham at lpsm.paris

<sup>‡</sup>EDF R&D & FiME xavier.warin at edf.fr

<sup>§</sup>EDF R&D, LPSM, Université de Paris mgermain at lpsm.paris

In this article, we introduce a numerical method based on machine learning techniques and backward in time iterations, which extends the proposed schemes in [VSS18] for linear problems, and in the recent work [HPW19] for semi-linear PDEs. The approach in these works consists in estimating simultaneously the solution and its gradient by multi-layer neural networks by minimizing a sequence of loss functions defined in backward induction. A basic idea to extend this method to the fully nonlinear case would rely on the representation proposed in [Che+07]: at each time step  $t_n$  of an Euler scheme, the Hessian  $D_x^2 u$  at  $t_n$  is approximated by a neural network minimizing some local  $L_2$  criterion associated to a BSDE involving  $D_x u$  at date  $t_{n+1}$  and  $D_x^2 u$ . Then, the pair  $(u, D_x u)$  at date  $t_n$  is approximated/learned with a second minimization similarly as in the method described by [HPW19]. The first minimization can be implemented with different variations but numerical results show that the global scheme does not scale well with the dimension. Instability on the  $D_x^2 u$  calculation rapidly propagates during the backward resolution. Besides, the methodology appears to be costly when using two optimizations at each time step. An alternative approach that we develop here, is to combine the ideas of [HPW19] and the splitting method in [Bec+19] in order to derive a new deep learning scheme that requires only one local optimization during the backward resolution for learning the pair  $(u, D_x u)$  and approximating  $D_x^2 u$  by automatic differentiation of the gradient computed at the previous step.

The outline of the paper is organized as follows. In Section 2, we briefly recall the mathematical description of the classical feedforward approximation, and then derive the proposed neural networks-based backward scheme. We test our method in Section 3 on several various examples. First we illustrate our results with a PDE involving a non linearity of type  $uD_x^2 u$ . Then, we consider a stochastic linear quadratic problem with controlled volatility where an analytic solution is available, and we test the performance and accuracy of our algorithm up to dimension 20. Next, we apply our algorithm to a Monge-Ampère equation, and finally, we provide numerical tests for the solution to fully nonlinear Hamilton-Jacobi-Bellman equation, with nonlinearities of the form  $|D_x u|^2/D_x^2 u$ , arising in portfolio selection problem with stochastic volatilities.

## 2 The proposed deep backward scheme

Our aim is to numerically approximate the function  $u : [0, T] \times \mathbb{R}^d \mapsto \mathbb{R}$ , assumed to be the unique smooth solution to the fully nonlinear PDE (1.1) under suitable conditions. This will be achieved by means of neural networks approximations for  $u$  and its gradient  $D_x u$ , relying on a backward scheme and training simulated data of some forward diffusion process. Approximations of PDE in high dimension by neural networks have now become quite popular, and are supported theoretically by recent results in [Hut+18] and [DLM19] showing their efficiency to overcome the curse of dimensionality.

### 2.1 Feedforward neural network to approximate functions

We denote by  $d_0$  the dimension of the input variables, and  $d_1$  the dimension of the output variable. A (deep) neural network is characterized by a number of layers  $L + 1 \in \mathbb{N} \setminus \{1, 2\}$  with  $m_\ell$ ,  $\ell = 0, \dots, L$ , the number of neurons (units or nodes) on each layer: the first layer is the input layer with  $m_0 = d$ , the last layer is the output layer with  $m_L = d_1$ , and the  $L - 1$  layers between are called hidden layers, where we choose for simplicity the same dimension  $m_\ell = m$ ,  $\ell = 1, \dots, L - 1$ .

A feedforward neural network is a function from  $\mathbb{R}^{d_0}$  to  $\mathbb{R}^{d_1}$  defined as the composition

$$x \in \mathbb{R}^d \mapsto A_L \circ \varrho \circ A_{L-1} \circ \dots \circ \varrho \circ A_1(x) \in \mathbb{R}. \quad (2.1)$$

Here  $A_\ell$ ,  $\ell = 1, \dots, L$  are affine transformations:  $A_1$  maps from  $\mathbb{R}^{d_0}$  to  $\mathbb{R}^m$ ,  $A_2, \dots, A_{L-1}$  map from  $\mathbb{R}^m$  to  $\mathbb{R}^m$ , and  $A_L$  maps from  $\mathbb{R}^m$  to  $\mathbb{R}^{d_1}$ , represented by

$$A_\ell(x) = \mathcal{W}_\ell x + \beta_\ell,$$

for a matrix  $\mathcal{W}_\ell$  called weight, and a vector  $\beta_\ell$  called bias term,  $\varrho : \mathbb{R} \rightarrow \mathbb{R}$  is a nonlinear function, called activation function, and applied component-wise on the outputs of  $A_\ell$ , i.e.,  $\varrho(x_1, \dots, x_m) = (\varrho(x_1), \dots, \varrho(x_m))$ . Standard examples of activation functions are the sigmoid, the ReLu, the Elu, tanh.

All these matrices  $\mathcal{W}_\ell$  and vectors  $\beta_\ell$ ,  $\ell = 1, \dots, L$ , are the parameters of the neural network, and can be identified with an element  $\theta \in \mathbb{R}^{N_m}$ , where  $N_m = \sum_{\ell=0}^{L-1} m_\ell(1+m_{\ell+1}) = d_0(1+m) + m(1+m)(L-2) + m(1+d_1)$  is the number of parameters. We denote by  $\mathcal{N}_{d_0, d_1, L, m}$  the set of all functions generated by (2.1) for  $\theta \in \mathbb{R}^{N_m}$ .

### 2.2 Forward-backward representation

Let us introduce a forward diffusion process

$$X_t = X_0 + \int_0^t \mu(s, X_s) ds + \int_0^t \sigma(s, X_s) dW_s, \quad 0 \leq t \leq T, \quad (2.2)$$

where  $\mu$  is a function defined on  $[0, T] \times \mathbb{R}^d$  with values in  $\mathbb{R}^d$ ,  $\sigma$  is a function defined on  $[0, T] \times \mathbb{R}^d$  with values in  $\mathbb{M}^d$  the set of  $d \times d$  matrices, and  $W$  a  $d$ -dimensional Brownian motion on some probability space  $(\Omega, \mathcal{F}, \mathbb{P})$  equipped with a filtration  $\mathbb{F} = (\mathcal{F}_t)_{0 \leq t \leq T}$  satisfying the usual conditions. The process  $X$  will be used for the simulation of training data in our deep learning algorithm, and we shall discuss later the choice of the drift and diffusion coefficients  $\mu$  and  $\sigma$ , see Remark 2.2.

Let us next denote by  $(Y, Z, \Gamma)$  the triple of  $\mathbb{F}$ -adapted processes valued in  $\mathbb{R} \times \mathbb{R}^d \times \mathbb{S}^d$ , defined by

$$Y_t = u(t, X_t), \quad Z_t = D_x u(t, X_t), \quad \Gamma_t = D_x^2 u(t, X_t), \quad 0 \leq t \leq T. \quad (2.3)$$

By Itô's formula applied to  $u(t, X_t)$ , and since  $u$  is solution to (1.1), we see that  $(Y, Z, \Gamma)$  satisfies the backward equation:

$$\begin{aligned} Y_t &= g(X_T) - \int_t^T [\mu(s, X_s) \cdot Z_s + \frac{1}{2} \text{tr}(\sigma \sigma^\top(s, X_s) \Gamma_s) - f(s, X_s, Y_s, Z_s, \Gamma_s)] ds \\ &\quad - \int_t^T \sigma^\top(s, X_s) Z_s \cdot dW_s, \quad 0 \leq t \leq T. \end{aligned} \quad (2.4)$$

## 2.3 Algorithm

We now provide a numerical approximation of the forward backward system (2.2)-(2.4), and consequently of the solution  $u$  (as well as its gradient  $D_x u$ ) to the PDE (1.1).

We start from a time grid  $\pi = \{t_i, i = 0, \dots, N\}$  of  $[0, T]$ , with  $t_0 = 0 < t_1 < \dots < t_N = T$ , and time steps  $\Delta t_i := t_{i+1} - t_i, i = 0, \dots, N-1$ . The time discretization of the forward process  $X$  on  $\pi$  is then equal (typically when  $\mu$  and  $\sigma$  are constants) or approximated by an Euler scheme:

$$X_{t_{i+1}} = X_{t_i} + \mu(t_i, X_{t_i}) \Delta t_i + \sigma(t_i, X_{t_i}) \Delta W_{t_i}, \quad i = 0, \dots, N-1,$$

where we set  $\Delta W_{t_i} := W_{t_{i+1}} - W_{t_i}$  (by misuse of notation, we keep the same notation  $X$  for the continuous time diffusion process and its Euler scheme). The backward SDE (2.4) is approximated by the time discretized scheme

$$Y_{t_i} \simeq Y_{t_{i+1}} - [\mu(t_i, X_{t_i}) \cdot Z_{t_i} + \frac{1}{2} \text{tr}(\sigma \sigma^\top(t_i, X_{t_i}) \Gamma_{t_i}) - f(t_i, X_{t_i}, Y_{t_i}, Z_{t_i}, \Gamma_{t_i})] \Delta t_i - \sigma^\top(t_i, X_{t_i}) Z_{t_i} \cdot \Delta W_{t_i},$$

that is written in forward form as

$$Y_{t_{i+1}} \simeq F(t_i, X_{t_i}, Y_{t_i}, Z_{t_i}, \Gamma_{t_i}, \Delta t_i, \Delta W_{t_i}), \quad i = 0, \dots, N-1, \quad (2.5)$$

with

$$\begin{aligned} F(t, x, y, z, \gamma, h, \Delta) &:= y - \tilde{f}(t, x, y, z, \gamma) h + z^\top \sigma(t, x) \Delta, \\ \tilde{f}(t, x, y, z, \gamma) &:= f(t, x, y, z, \gamma) - \mu(t, x) \cdot z - \frac{1}{2} \text{tr}(\sigma \sigma^\top(t, x) \gamma). \end{aligned} \quad (2.6)$$

The idea of the proposed scheme is the following. Similarly as in [HPW19], we approximate at each time  $t_i, u(t_i, \cdot)$  and its gradient  $D_x u(t_i, \cdot)$ , by neural networks  $x \in \mathbb{R}^d \mapsto (\mathcal{U}_i(x; \theta), \mathcal{Z}_i(x; \theta))$  with parameter  $\theta$  that are learned optimally by backward induction: suppose that  $\hat{\mathcal{U}}_{i+1} := \mathcal{U}_{i+1}(\cdot; \theta_{i+1}^*), \hat{\mathcal{Z}}_{i+1} := \mathcal{Z}_{i+1}(\cdot; \theta_{i+1}^*)$  is an approximation of  $u(t_{i+1}, \cdot)$  and  $D_x u(t_{i+1}, \cdot)$  at time  $t_{i+1}$ , then  $\theta_i^*$  is computed from the minimization of the quadratic loss function:

$$\hat{L}_i(\theta) = \mathbb{E} \left| \hat{\mathcal{U}}_{i+1} - F(t_i, X_{t_i}, \mathcal{U}_i(X_{t_i}; \theta), \mathcal{Z}_i(X_{t_i}; \theta), D \hat{\mathcal{Z}}_{i+1}(\mathcal{T}(X_{t_{i+1}})), \Delta t_i, \Delta W_{t_i}) \right|^2$$

where  $\mathcal{T}$  is a truncation operator such that  $\mathcal{T}(X)$  is bounded for example by a quantile of the diffusion process and  $D \hat{\mathcal{Z}}_{i+1}$  stands for the automatic differentiation of  $\hat{\mathcal{Z}}_{i+1}$ . The truncation permits to avoid that the oscillations of the neural network fit in zone where the simulations propagate scarcely to areas of importance. This truncation may be necessary to get convergence on some rather difficult cases.

The intuition for the relevance of this scheme to the approximation of the PDE (1.1) is the following. From (2.3) and (2.5), the solution  $u$  to (1.1) should approximately satisfy

$$u(t_{i+1}, X_{t_{i+1}}) \simeq F(t_i, X_{t_i}, u(t_i, X_{t_i}), D_x u(t_i, X_{t_i}), D_x^2 u(t_i, X_{t_i}), \Delta t_i, \Delta W_{t_i}).$$

Suppose that at time  $t_{i+1}, \hat{\mathcal{U}}_{i+1}$  is an estimation of  $u(t_{i+1}, \cdot)$ . Recalling the expression of  $F$  in (2.6), the quadratic loss function at time  $t_i$  is then approximately equal to

$$\begin{aligned} \hat{L}_i(\theta) &\simeq \mathbb{E} \left| u(t_i, X_{t_i}) - \mathcal{U}_i(X_{t_i}; \theta) + (D_x u(t_i, X_{t_i}) - \mathcal{Z}_i(X_{t_i}; \theta))^\top \sigma(t_i, X_{t_i}) \Delta W_{t_i} \right. \\ &\quad \left. - \Delta t_i [\tilde{f}(t_i, X_{t_i}, u(t_i, X_{t_i}), D_x u(t_i, X_{t_i}), D_x^2 u(t_i, X_{t_i})) - \tilde{f}(t_i, X_{t_i}, \mathcal{U}_i(X_{t_i}; \theta), \mathcal{Z}_i(X_{t_i}; \theta), D \hat{\mathcal{Z}}_{i+1}(\mathcal{T}(X_{t_{i+1}})))] \right|^2. \end{aligned}$$

By assuming that  $\tilde{f}$  has small nonlinearities in its arguments  $(y, z, \gamma)$ , say Lipschitz, possibly with a suitable choice of  $\mu, \sigma$ , the loss function is thus approximately equal to

$$\hat{L}_i(\theta) \simeq (1 + O(\Delta t_i)) \mathbb{E} |u(t_i, X_{t_i}) - \mathcal{U}_i(X_{t_i}; \theta)|^2 + O(\Delta t_i) \mathbb{E} |D_x u(t_i, X_{t_i}) - \mathcal{Z}_i(X_{t_i}; \theta)|^2 + O(|\Delta t_i|^2).$$

Therefore, by minimizing over  $\theta$  this quadratic loss function, via stochastic gradient descent (SGD) based on simulations of  $(X_{t_i}, X_{t_{i+1}}, \Delta W_{t_i})$  (called training data in the machine learning language), one expects the neural networks  $\mathcal{U}_i$  and  $\mathcal{Z}_i$  to learn/approximate better and better the functions  $u(t_i, \cdot)$  and  $D_x u(t_i, \cdot)$  in view of the universal approximation theorem for neural networks. The rigorous convergence of this algorithm is postponed to a future work.

To sum up, the global algorithm is given in Algo 1 in the case where  $g$  is Lipschitz and the derivative can be analytically calculated almost everywhere. If the derivative of  $g$  is not available, it can be calculated by automatic differentiation of the neural network approximation of  $g$ .

---

**Algorithm 1** Algorithm for fully non linear equations.

---

1: Use a single deep neural network  $(\mathcal{U}_N(\cdot; \theta), \mathcal{Z}_N(\cdot; \theta)) \in \mathcal{N}_{d,1+d,L,m}$  and minimize (by SGD)

$$\begin{cases} \hat{L}_N(\theta) := \mathbb{E} |\mathcal{U}_N(X_{t_N}; \theta) - g(X_{t_N})|^2 + \frac{\Delta t_{N-1}}{d} \mathbb{E} |\mathcal{Z}_N(X_{t_N}; \theta) - Dg(X_{t_N})|^2 \\ \theta_N^* \in \arg \min_{\theta \in \mathbb{R}^{N_m}} \hat{L}_N(\theta). \end{cases}$$

2:  $\hat{\mathcal{U}}_N = \mathcal{U}_N(\cdot; \theta_N^*)$ , and set  $\hat{\mathcal{Z}}_N = \mathcal{Z}_N(\cdot; \theta_N^*)$

3: **for**  $i = N - 1, \dots, 0$  **do**

4: Use a single deep neural network  $(\mathcal{U}_i(\cdot; \theta), \mathcal{Z}_i(\cdot; \theta)) \in \mathcal{N}_{d,1+d,L,m}$  for the approximation of  $(u(t_i, \cdot), D_x u(t_i, \cdot))$ , and compute (by SGD) the minimizer of the expected quadratic loss function

$$\begin{cases} \hat{L}_i(\theta) := \mathbb{E} \left| \hat{\mathcal{U}}_{i+1}(X_{t_{i+1}}) - F(t_i, X_{t_i}, \mathcal{U}_i(X_{t_i}; \theta), \mathcal{Z}_i(X_{t_i}; \theta), D\hat{\mathcal{Z}}_{i+1}(\mathcal{T}(X_{t_{i+1}})), \Delta t_i, \Delta W_{t_i}) \right|^2 \\ \theta_i^* \in \arg \min_{\theta \in \mathbb{R}^{N_m}} \hat{L}_i(\theta). \end{cases} \quad (2.7)$$

5: Update:  $\hat{\mathcal{U}}_i = \mathcal{U}_i(\cdot; \theta_i^*)$ , and set  $\hat{\mathcal{Z}}_i = \mathcal{Z}_i(\cdot; \theta_i^*)$ .

---

**Remark 2.1** A variation in the algorithm consists in using two neural networks for  $\hat{\mathcal{U}}_i$  and  $\hat{\mathcal{Z}}_i$  instead of one.  $\square$

**Remark 2.2** The diffusion process  $X$  is used for the training simulations in the stochastic gradient descent method for finding the minimizer of the quadratic loss function in (2.7), where the expectation is replaced by empirical average for numerical implementation. The choice of the drift coefficient is typically related to the underlying probabilistic problem associated to the PDE (for example a stochastic control problem), but does not really matter. The choice of the diffusion coefficient  $\sigma$  is more delicate: large  $\sigma$  induces a better exploration of the state space, but would require a lot of neurons. Moreover, for the applications in stochastic control, we might explore some region that are visited with very small probabilities by the optimal state process, hence representing few interest. On the other hand, small  $\sigma$  means a weak exploration, and we might lack information and precision on some region of the state space. In practice and for the numerical examples in the next section, we test the scheme for different  $\sigma$  and by varying the number of time steps, and if it converges to the same solution, one can consider that we have obtained the correct solution.  $\square$

### 3 Numerical results

We first construct an example with different non linearities in the Hessian term and the solution. We graphically show that the solution is very well calculated in dimension one and then move to higher dimensions. We then use an example derived from a stochastic optimization problem with an analytic solution and show that we are able to accurately calculate the solution. Next, we consider the numerical resolution of the Monge-Ampère equation, and finally, give some tests for a fully nonlinear Hamilton-Jacobi-Bellman equation arising from portfolio optimization with stochastic volatilities.

In the whole numerical part, we use a classical Feed Forward Network using layers with  $n$  neurons each and a tanh activation function, the output layer uses an identity activation function. At each time step the resolution of equation (2.7) is achieved using some mini-batch with 1000 trajectories. Every 50 inner iterations the convergence rate is checked using 10000 trajectories and an adaptation of the learning rate is achieved using an Adam gradient descent, see [KB14]. Notice that the adaptation of the learning rate is not common with the

Adam method but in our case it appears to be crucial to have a steady diminution of the loss of the objective function. The procedure is described in [CWNMW19] and the parameters chosen are the same as in this article.

During time resolution, it is far more effective to initialize the solution of equations (2.7) with the solution  $(\mathcal{U}, \mathcal{Z})$  at the next time step. The number of outer iterations is fixed for each optimization. It is set to 500 for the first optimization at date  $N$  and then a value of 100 outer iteration is used at the dates  $i < N$ . At the first time step, the learning rate is taken equal to  $1E - 2$  and at the following time steps, we start with a learning rate equal to  $1E - 3$ . All experiments have achieved using Tensorflow [Aba+15]. In the sequel, the PDE solutions on curves are calculated as the average of 10 runs. We provide some standard deviation observed for some results. We also show the impact of the choice of the diffusion coefficient  $\sigma$ , and the influence of the number of neurons on the accuracy of the results.

### 3.1 A non linearity in $uD_x^2u$

We consider a generator in the form

$$f(t, x, y, z, \gamma) = y \text{tr}(\gamma) + \frac{y}{2} + 2y^2 - 2y^4 e^{-(T-t)},$$

and  $g(x) = \tanh\left(\frac{\sum_{i=1}^d x_i}{\sqrt{d}}\right)$ , so that an analytical solution is available:

$$u(t, x) = \tanh\left(\frac{\sum_{i=1}^d x_i}{\sqrt{d}}\right) e^{-\frac{T-t}{2}}.$$

We fix the horizon  $T = 1$ , and choose to evaluate the solution at  $t = 0$  and  $x = 0.5 \frac{\mathbf{1}_d}{\sqrt{d}}$  (here  $\mathbf{1}_d$  denotes the vector in  $\mathbb{R}^d$  with all components equal to 1), for which  $u(t, x) = 0.761902$  while its derivative is equal to 1.2966. This initial value  $x$  is chosen such that independently of the dimension the solution is varying around this point and not in a region where the tanh function is close to  $-1$  or  $1$ .

The coefficients of the forward process used to solve the equation are

$$\sigma = \frac{\hat{\sigma}}{\sqrt{d}} \mathbf{I}_d, \quad \mu = 0,$$

(here  $\mathbf{I}_d$  is the identity  $d \times d$ -matrix) and the truncation operator indexed by a parameter  $p$  is chosen equal to

$$\mathcal{T}_p(X_t^{0,x}) = \min \{ \max[x - \sigma \sqrt{t} \phi_p, X_t^{0,x}], x + \sigma \sqrt{t} \phi_p \},$$

where  $\phi_p = \mathcal{N}^{-1}(p)$ ,  $\mathcal{N}$  is the CDF of a unit centered Gaussian random variable. In the numerical results we take  $p = 0.999$  and  $n = 20$  neurons.

We first begin in dimension one, and show in figure 1 how  $u$ ,  $D_x u$  and  $D_x^2 u$  are well approximated by the resolution method.

On figure 2, we check the convergence, for different values of  $\hat{\sigma}$  of both the value function and its derivative at point  $x$  and date 0. Standard deviation of the function value is very low and the standard deviation of the derivative still being low.

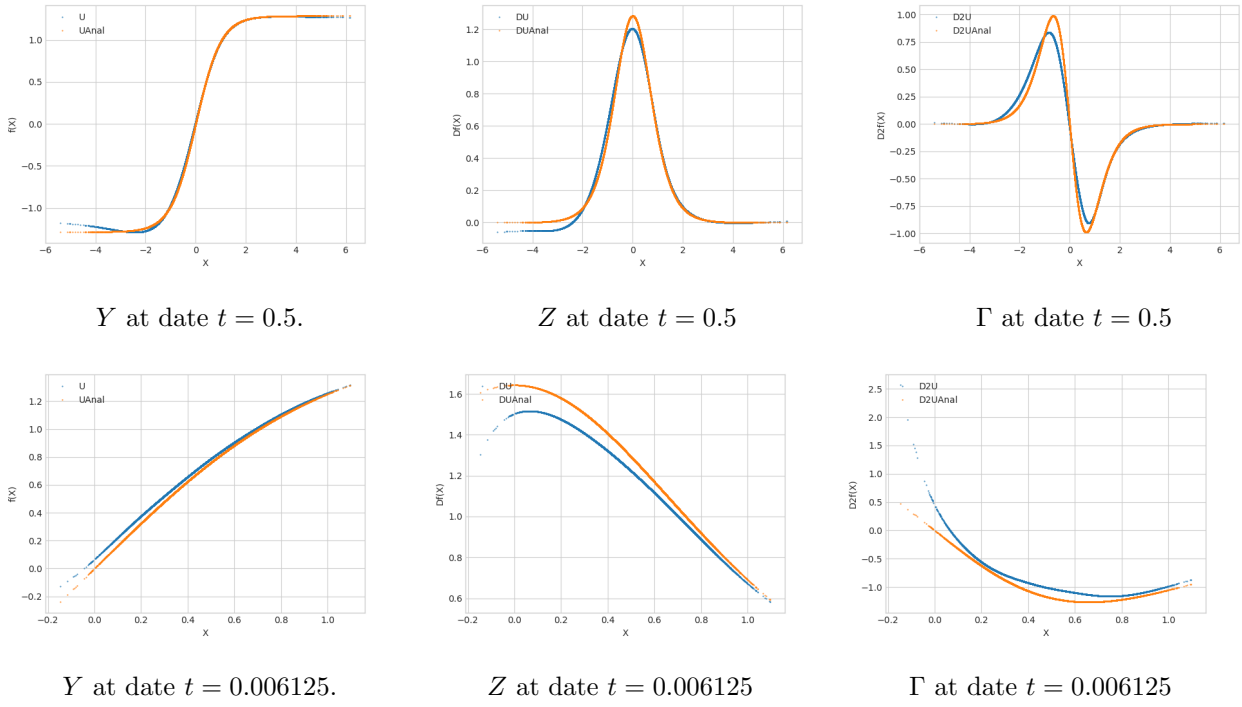


Figure 1: A single valuation run for test case one 1D using 160 time steps,  $\hat{\sigma} = 2.$ ,  $p = 0.999$ , 20 neurons, 2 layers.

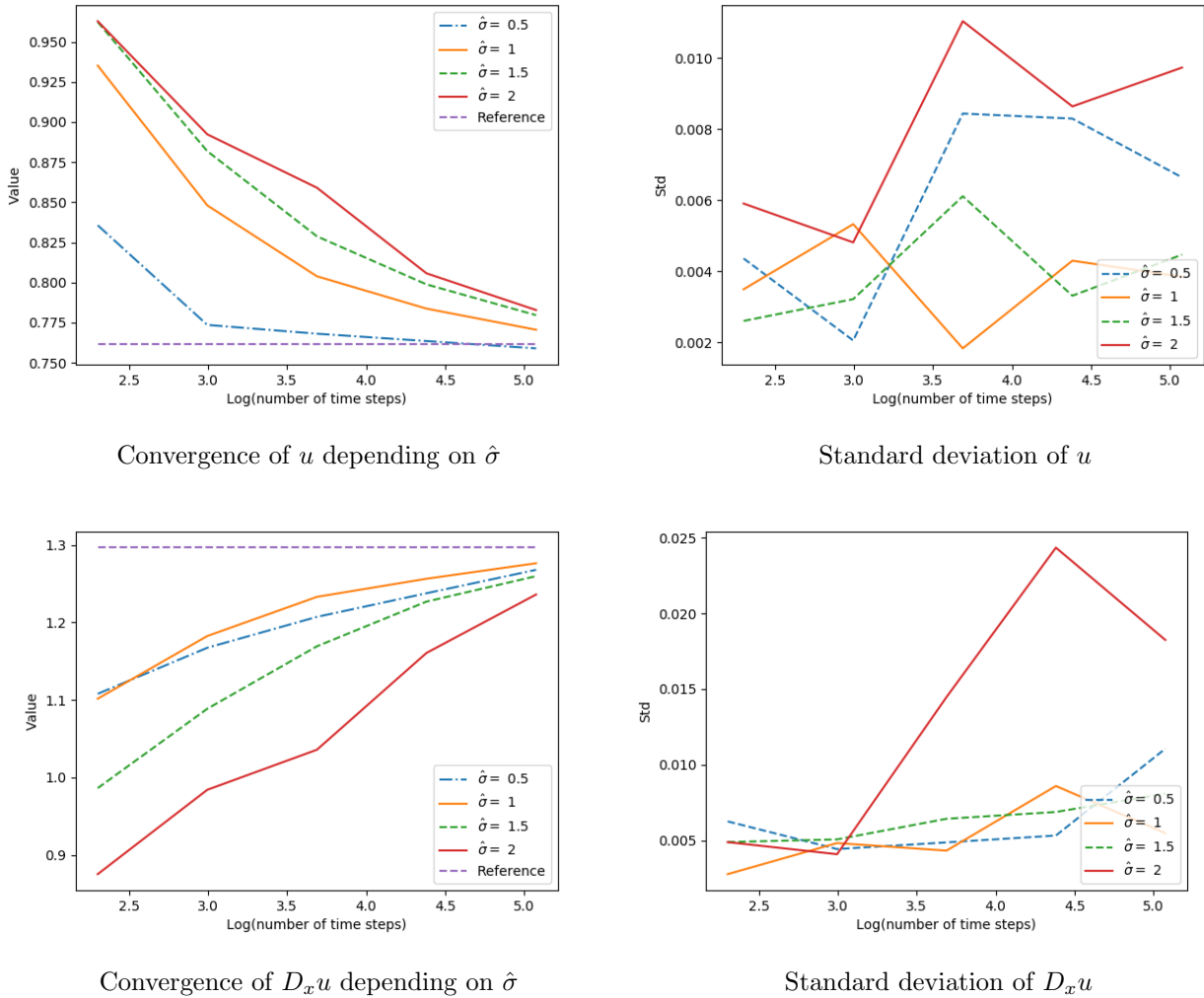
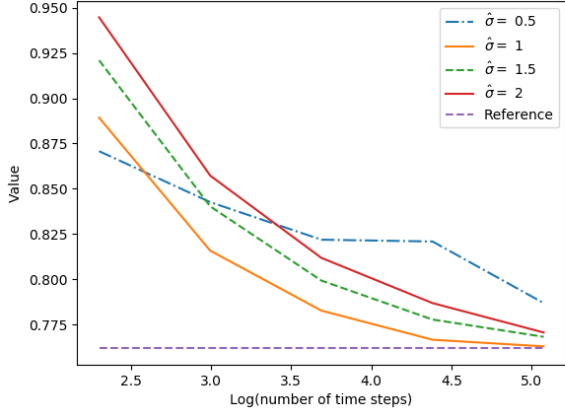
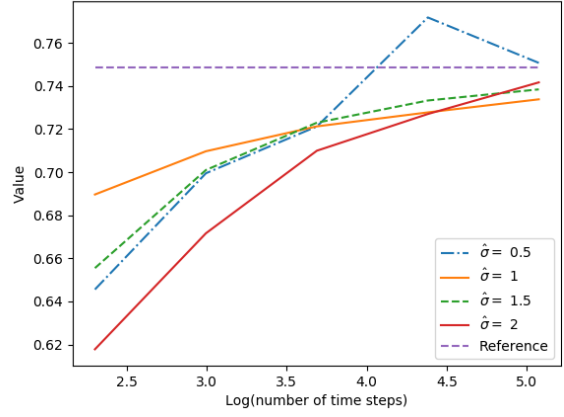


Figure 2: Convergence in 1D of the case one, number of neurons par layer equal to 20, 2 layers,  $p = 0.999$ .

As the dimension increases, we have to increase the value of  $\hat{\sigma}$  of the forward process. In dimension 3, the value  $\hat{\sigma} = 0.5$  gives high standard deviation in the result obtained as shown on figure 3, while in dimension 10, see Figure 4, we see that the value  $\hat{\sigma} = 1$  is too low to give good results. We also clearly notice that in 10D, a smaller time step should be used but in our test cases we decided to consider a maximum number of time steps equal to 160.

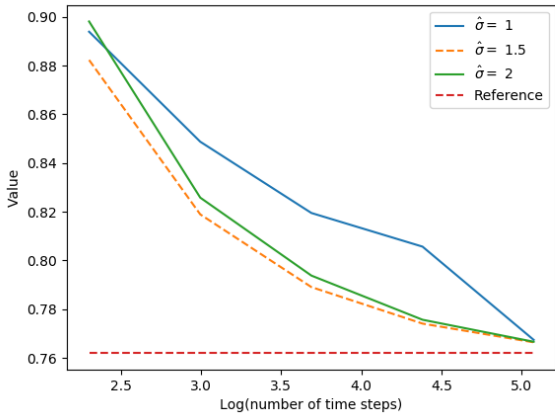


Convergence of  $u$  depending on  $\hat{\sigma}$

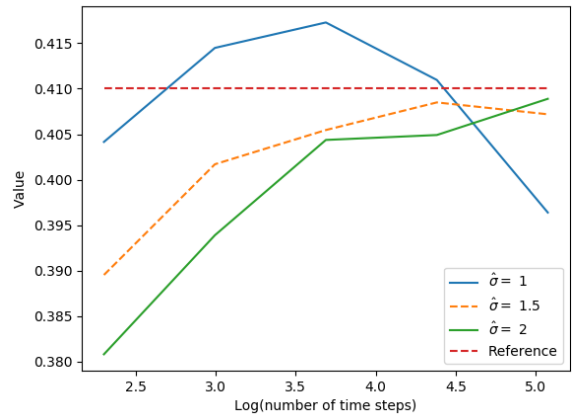


Convergence of  $D_x u$  (first component) depending on  $\hat{\sigma}$

Figure 3: Convergence in 3D of the case one, number of neurons par layer equal to 20, 2 layers,  $p = 0.999$ .



Convergence of  $u$  depending on  $\hat{\sigma}$



Convergence of  $D_x u$  depending on  $\hat{\sigma}$  (first component)

Figure 4: Convergence in 10D of the case one, number of neurons par layer equal to 20, 2 layers,  $p = 0.999$ .

On this simple test case, the dimension is not a problem and very good results are obtained in dimension 20 or above with only 20 neurons and 2 layers.



### 3.2 A linear quadratic stochastic test case.

In this example, we consider a controlled process  $\mathcal{X} = \mathcal{X}^\alpha$  with dynamics in  $\mathbb{R}^d$  according to

$$d\mathcal{X}_t = (A\mathcal{X}_t + B\alpha_t)dt + D\alpha_t dW_t, \quad 0 \leq t \leq T, \quad \mathcal{X}_0 = x,$$

where  $W$  is a real Brownian motion, the control process  $\alpha$  is valued in  $\mathbb{R}$ , and the constant coefficients  $A \in \mathbb{M}^d$ ,  $B \in \mathbb{R}^d$ ,  $D \in \mathbb{R}^d$ . The quadratic cost functional to be minimized is

$$J(\alpha) = \mathbb{E} \left[ \int_0^T (\mathcal{X}_t^\top Q \mathcal{X}_t + \alpha_t^2 N) dt + \mathcal{X}_T^\top P \mathcal{X}_T \right],$$

where  $P, Q$  are non negative  $d \times d$  symmetric matrices and  $N \in \mathbb{R}$  is strictly positive.

The Bellman equation associated to this stochastic control problem is:

$$\begin{aligned} \frac{\partial u}{\partial t} + \inf_{a \in \mathbb{R}} [(Ax + Ba) \cdot D_x u + \frac{a^2}{2} \text{tr}(DD^\top D_x^2 u) + x^\top Q x + Na^2] &= 0, \quad (t, x) \in [0, T) \times \mathbb{R}^d, \\ u(T, x) &= x^\top P x, \quad x \in \mathbb{R}^d, \end{aligned}$$

which can be rewritten as a fully nonlinear equation in the form (1.1) with

$$f(t, x, y, z, \gamma) = x^\top Q x + Ax \cdot z - \frac{1}{2} \frac{|B^\top z|^2}{\text{tr}(DD^\top \gamma) + 2N}.$$

An explicit solution to this PDE is given by

$$u(t, x) = x^\top K(t)x,$$

where  $K(t)$  is non negative  $d \times d$  symmetric matrix function solution to the Riccati equation:

$$\dot{K} + A^\top K + KA + Q - \frac{KBB^\top K}{N + D^\top KD} = 0, \quad K(T) = P.$$

We take  $T = 1$ . The coefficients of the forward process used to solve the equation are

$$\sigma = \frac{\hat{\sigma}}{\sqrt{d}} \mathbf{I}_d, \quad \mu(t, x) = Ax.$$

In our numerical example we take the following parameters for the optimization problem:

$$A = \mathbf{I}_d, \quad B = D = \mathbf{1}_d, \quad Q = P = \frac{1}{d} \mathbf{I}_d, \quad N = d$$

and we want to estimate the solution at  $x = \mathbf{1}_d$ .

In this example, the truncation operator (indexed by  $p$  between 0 and 1 and close to 1) is as follows:

$$\mathcal{T}_p(X_t^x) = \min \left\{ \max \left[ x e^{\hat{A}t} - \sigma \sqrt{\frac{e^{2\hat{A}t} - \hat{\mathbf{1}}}{2\hat{A}}} \phi_p, X_t^x \right], x e^{\hat{A}t} + \sigma \sqrt{\frac{e^{2\hat{A}t} - \hat{\mathbf{1}}}{2\hat{A}}} \phi_p \right\},$$

where  $\phi_p = \mathcal{N}^{-1}(p)$ ,  $\hat{A}$  is a vector so that  $\hat{A}_i = A_{ii}$ ,  $i = 1, \dots, d$ ,  $\hat{\mathbf{1}}$  is a unit vector, and the square root is taken componentwise.

On figure 5 we give the solution of the PDE using  $\hat{\sigma} = 1.5$  obtained for two dates: at  $t = 0.5$  and at  $t$  close to zero. We observe that we have a very good estimation of the function value and a correct one of the  $\Gamma$  value at date  $t = 0.5$ . The precision remains good for  $\Gamma$  close to  $t = 0$  and very good for  $u$  and  $D_x u$ .

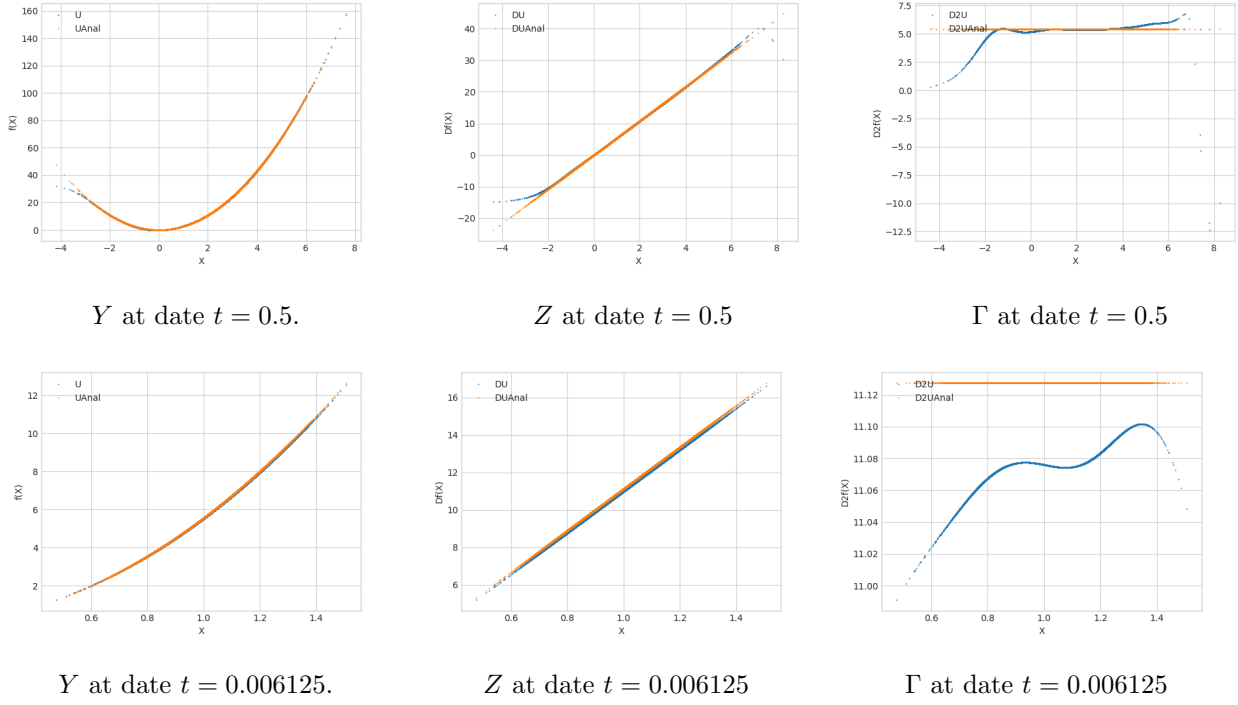


Figure 5: Test case linear quadratic 1D using 160 time steps,  $\hat{\sigma} = 1.5$ ,  $p = 0.999$ , 100 neurons.

On figures 6, we give the results obtained in dimension one by varying  $\hat{\sigma}$ . For a value of  $\hat{\sigma} = 2$ , the standard deviation of the result becomes far higher than with  $\hat{\sigma} = 0.5$  or 1.

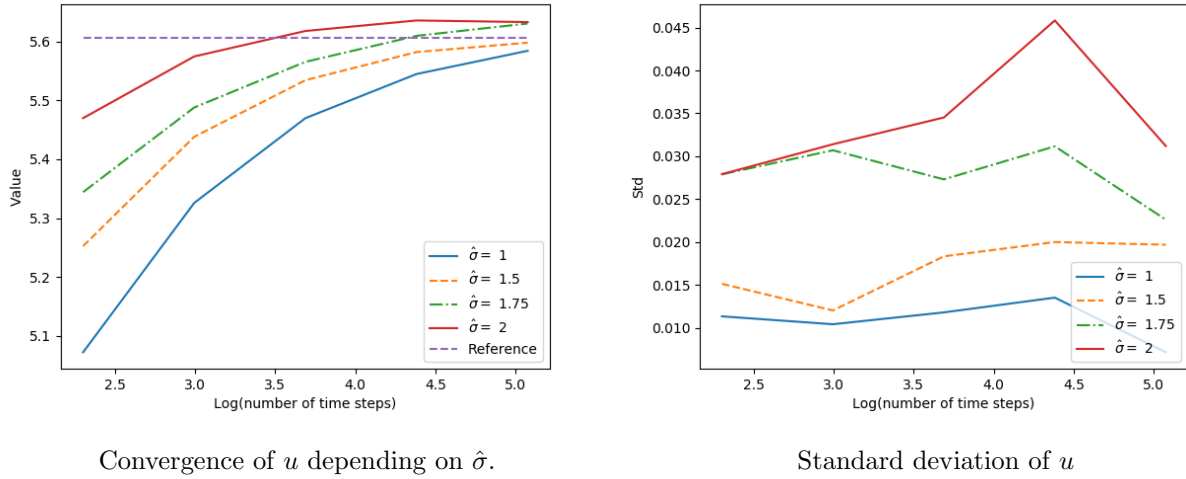
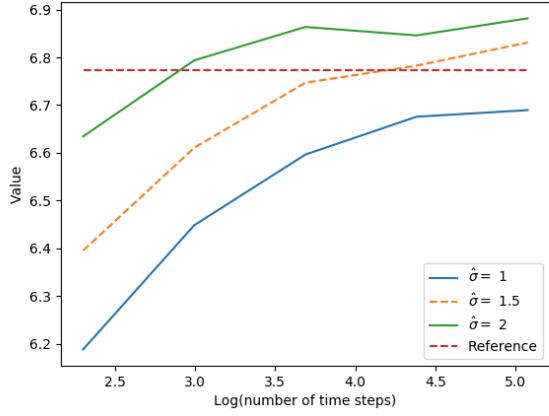
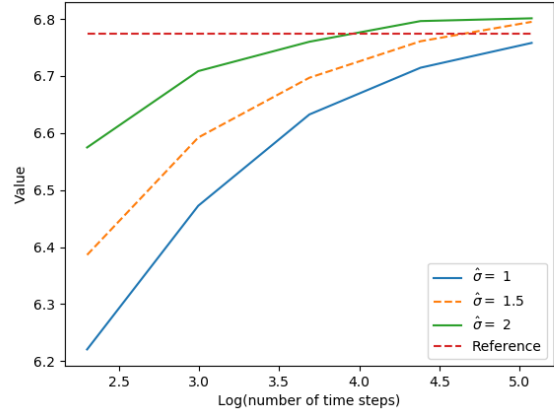


Figure 6: Convergence in 1D of the linear quadratic case, number of neurons per layer equal to 50, 2 layers,  $p = 0.999$ .

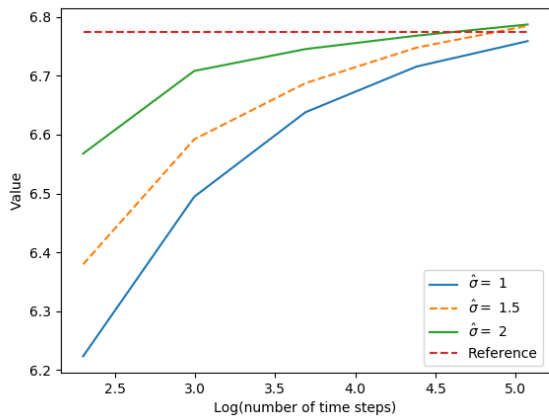
On figure 7, we take a quite low truncation factor  $p = 0.95$  and observe that the number of neurons to take has to be rather high. We have also checked that taking a number of hidden layers equal to 3 does not improve the results.



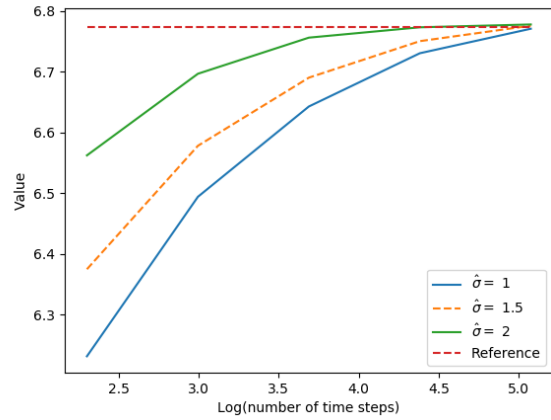
10 neurons



20 neurons



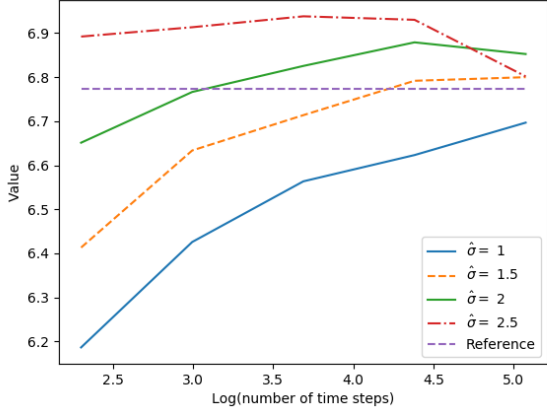
30 neurons



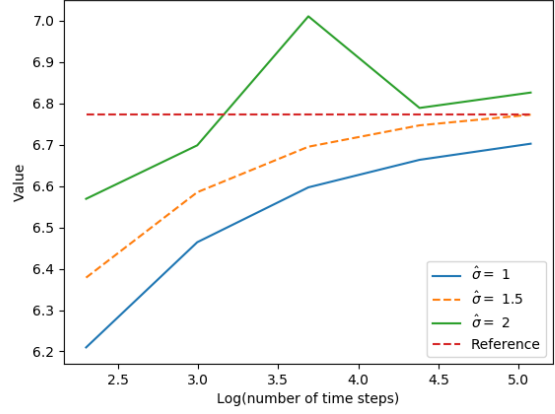
50 neurons

Figure 7: Convergence in 3D of the linear quadratic case, 2 layers, testing the influence of the number of neurons, truncation  $p = 0.95$ .

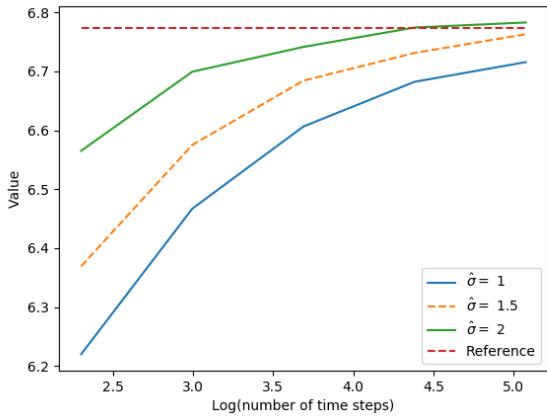
On figure 8, we give the same graphs for a truncation factor higher. As we take a higher truncation factor the number of neurons to use has to be increased to 100.



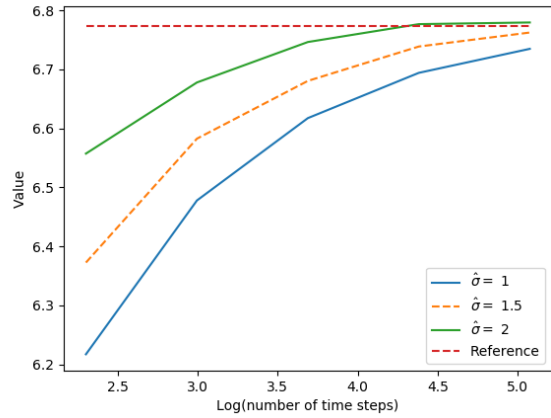
10 neurons



20 neurons



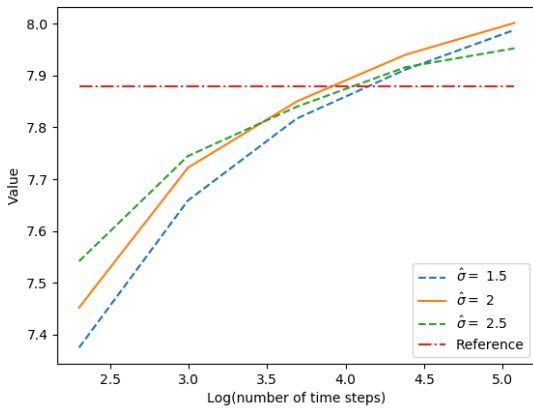
50 neurons



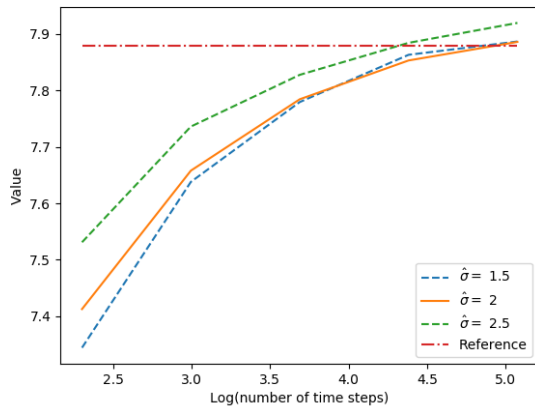
100 neurons

Figure 8: Convergence in 3D of the linear quadratic case, 2 layers, testing the influence of the number of neurons, truncation  $p = 0.99$ .

On figure 9, we observe in dimension 7 the influence of the number of neurons on the result for a high truncation factor  $p = 0.999$ . With a number of neurons equal to 50, we clearly have a bias disappearing with a number of neurons equal to 100. We had to take higher values of  $\hat{\sigma}$  to get good results.



Convergence with 50 neurons



Convergence with 100 neurons

Figure 9: Convergence in 7D of the linear quadratic case, 2 layers,  $p = 0.999$ .

On figure 10, we check that influence of the truncation factor appears to be slow for higher dimensions.

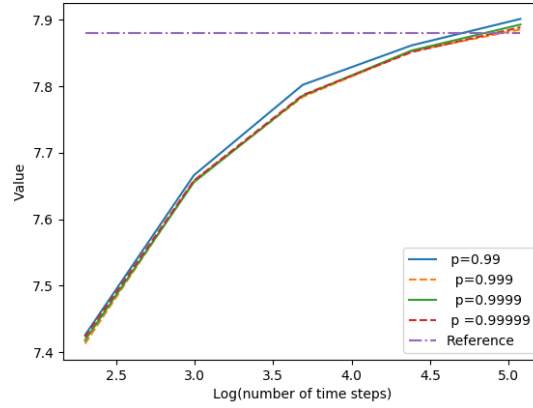


Figure 10: Function value convergence in 7D of the linear quadratic case with 2 layers, 100 neurons, testing  $p$ .

Finally, we give results in dimension 10, 15 and 20 for  $p = 0.999$  on figures 11, 12. We observe that the number a neurons with 2 hidden layers has to increase with the dimension but also that the increase is rather slow in contrast with the case of one hidden layer as theoretically shown in [Pin99]. For  $\hat{\sigma} = 5$  we had to take 300 neurons to get very accurate results.

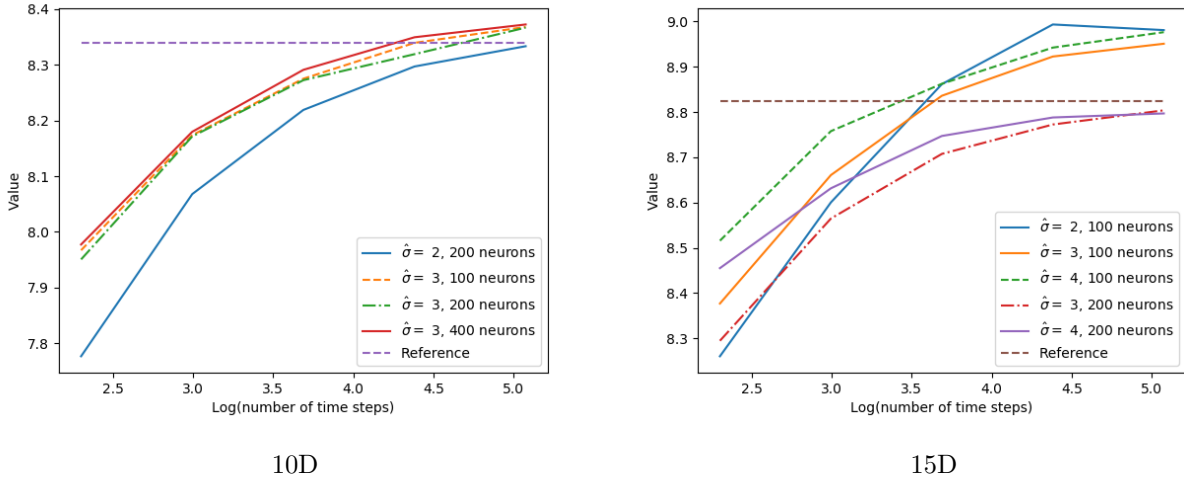


Figure 11: Function value convergence in 10D and 15D of the linear quadratic case with 2 layers,  $p = 0.999$ .

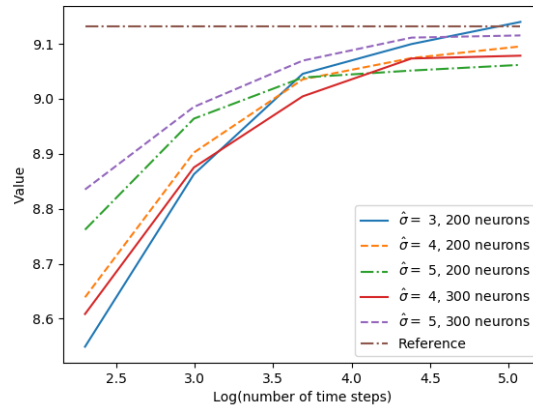


Figure 12: Function value convergence in 20D of the linear quadratic case with 2 layers,  $p = 0.999$ .

### 3.3 Monge-Ampère equation

Let us consider the parabolic Monge-Ampère equation

$$\begin{cases} \partial_t u + \det(D_x^2 u) = h(x), & (t, x) \in [0, T] \times \mathbb{R}^d, \\ u(T, x) = g(x), \end{cases} \quad (3.1)$$

where  $\det(D_x^2 u)$  is the determinant of the Hessian matrix  $D_x^2 u$ . It is in the form (1.1) with

$$f(t, x, \gamma) = \det(\gamma) - h(x).$$

We test our algorithm by choosing a  $C^2$  function  $g$ , then compute  $G = \det(D_x^2 g)$ , and set  $h := G - 1$ . Then, by construction, the function

$$u(t, x) = g(x) + T - t,$$

is solution to the Monge-Ampère equation (3.1). We choose  $g(x) = \cos(\sum_{i=1}^d x_i / \sqrt{d})$ , and we shall train with the forward process  $X = x_0 + W$ , where  $W$  is a  $d$ -dimensional Brownian motion. On this example, we use neural networks with 3 hidden layers,  $d + 10$  neurons per layer, and we do not need to apply any truncation to the forward process  $X$ . Actually, we observe that adding a truncation worsens the results.

The following tables give the results in dimension  $d = 5, 8$  and  $15$ , and for  $T = 1$ .

Averaged value	Standard deviation	Relative error (%)
0.37901	0.00312	0.97

Figure 13: Estimate of  $u(0, x_0 = 1_5)$  on the Monge Ampere problem (3.1) ( $d = 5$ ) with  $N = 120$ . Average and standard deviation observed over 10 independent runs are reported. The theoretical solution is 0.38272712.

Averaged value	Standard deviation	Relative error (%)
0.25276	0.00235	1.17

Figure 14: Estimate of  $u(0, x_0 = 1_{15})$  on the Monge Ampere problem (3.1) ( $d = 15$ ) with  $N = 120$ . Average and standard deviation observed over 10 independent runs are reported. The theoretical solution is 0.25575373.

### 3.4 Portfolio selection

We consider a portfolio selection problem formulated as follows. There are  $n$  risky assets of uncorrelated price process  $P = (P^1, \dots, P^n)$  with dynamics

$$dP_t^i = P_t^i \sigma(V_t^i) [\lambda_i(V_t^i) dt + dW_t^i], \quad i = 1, \dots, n,$$

where  $W = (W^1, \dots, W^n)$  is a  $n$ -dimensional Brownian motion,  $b = (b^1, \dots, b^n)$  is the rate of return of the assets,  $\lambda = (\lambda^1, \dots, \lambda^n)$  is the risk premium of the assets,  $\sigma$  is a positive function (e.g.  $\sigma(v) = e^v$  corresponding to the Scott model), and  $V = (V^1, \dots, V^n)$  is the volatility factor modeled by an Ornstein-Uhlenbeck (O.U.) process

$$dV_t^i = \kappa_i [\theta_i - V_t^i] dt + \nu_i dB_t^i, \quad i = 1, \dots, n, \quad (3.2)$$

with  $\kappa_i, \theta_i, \nu_i > 0$ , and  $B = (B^1, \dots, B^n)$  a  $n$ -dimensional Brownian motion, s.t.  $d \langle W^i, B^j \rangle = \delta_{ij} \rho_{ij} dt$ , with  $\rho_i := \rho_{ii} \in (-1, 1)$ . An agent can invest at any time an amount  $\alpha_t = (\alpha_t^1, \dots, \alpha_t^n)$  in the stocks, which generates a wealth process  $\mathcal{X} = \mathcal{X}^\alpha$  governed by

$$d\mathcal{X}_t = \sum_{i=1}^n \alpha_t^i \sigma(V_t^i) [\lambda_i(V_t^i) dt + dW_t^i].$$

The objective of the agent is to maximize her expected utility from terminal wealth:

$$\mathbb{E}[U(\mathcal{X}_T^\alpha)] \leftarrow \text{maximize over } \alpha$$

It is well-known that the solution to this problem can be characterized by the dynamic programming method (see e.g. [Pha09]), which leads to the Hamilton-Jacobi-Bellman for the value function on  $[0, T] \times \mathbb{R} \times \mathbb{R}^n$ :

$$\begin{cases} \partial_t u + \sum_{i=1}^n [\kappa_i(\theta_i - v_i)\partial_{v_i} u + \frac{1}{2}\nu_i^2\partial_{v_i}^2 u] = \frac{1}{2}R(v)\frac{(\partial_x u)^2}{\partial_{xx}^2 u} + \sum_{i=1}^n [\rho_i\lambda_i(v_i)\nu_i\frac{\partial_x u\partial_{xv_i}^2 u}{\partial_{xx}^2 u} + \frac{1}{2}\rho_i^2\nu_i^2\frac{(\partial_{xv_i}^2 u)^2}{\partial_{xx}^2 u}] \\ u(T, x, v) = U(x), \quad x \in \mathbb{R}, v \in \mathbb{R}^n, \end{cases}$$

with a Sharpe ratio  $R(v) := |\lambda(v)|^2$ , for  $v = (v_1, \dots, v_n) \in (0, \infty)^n$ . The optimal portfolio strategy is then given in feedback form by  $\alpha_t^* = \hat{\alpha}(t, \mathcal{X}_t^*, V_t)$ , where  $\hat{\alpha} = (\hat{\alpha}_1, \dots, \hat{\alpha}_n)$  is given by

$$\hat{\alpha}_i(t, x, v) = -\frac{1}{\sigma(v_i)}\left(\lambda_i(v_i)\frac{\partial_x u}{\partial_{xx}^2 u} + \rho_i\nu_i\frac{\partial_{xv_i}^2 u}{\partial_{xx}^2 u}\right), \quad (t, x, v = (v_1, \dots, v_n)) \in [0, T] \times \mathbb{R} \times \mathbb{R}^n,$$

for  $i = 1, \dots, n$ . This Bellman equation is in the form (1.1) with

$$f(t, x, y, z, \gamma) = \sum_{i=1}^n [\kappa_i(\theta_i - v_i)z_i + \frac{1}{2}\nu_i^2\gamma_{ii}] - \frac{1}{2}R(v)\frac{z_0^2}{\gamma_{00}} - \sum_{i=1}^n [\rho_i\lambda_i(v_i)\nu_i\frac{z_0\gamma_{0i}}{\gamma_{00}} + \frac{1}{2}\rho_i^2\nu_i^2\frac{(\gamma_{0i})^2}{\gamma_{00}}],$$

for  $x = (x, v) \in \mathbb{R}^{n+1}$ ,  $z = (z_0, \dots, z_n) \in \mathbb{R}^{n+1}$ ,  $\gamma = (\gamma_{ij})_{0 \leq i, j \leq n} \in \mathbb{S}^{n+1}$ , and displays a high-nonlinearity in the Hessian argument  $\gamma$ .

The truncation operator indexed by a parameter  $p$  is chosen equal to

$$\mathcal{T}_p(X_t^{0,x}) = \min \{ \max[x - \sigma\sqrt{t}\phi_p, X_t^{0,x}], x + \sigma\sqrt{t}\phi_p \},$$

where  $\phi_p = \mathcal{N}^{-1}(p)$ ,  $\mathcal{N}$  is the CDF of a unit centered Gaussian random variable. In practice, we choose  $p = 0.95$ . We use neural networks with 2 hidden layers and  $d + 10$  neurons per layer. We shall test this example when the utility function  $U$  is of exponential form:  $U(x) = -\exp(-\eta x)$ , with  $\eta > 0$ , and under different cases for which closed-form solutions are available:

- (1) *Merton problem.* This corresponds to a degenerate case where the factor  $V$ , hence the volatility  $\sigma$  and the risk premium  $\lambda$  are constant, so that the generator of Bellman equation reduces to

$$f(t, x, y, z, \gamma) = -\frac{1}{2}|\lambda|^2\frac{z^2}{\gamma}, \quad (t, x, y, z) \in [0, T] \times \mathbb{R} \times \mathbb{R} \times \mathbb{R}, \quad (3.3)$$

with explicit solution given by:

$$u(t, x) = e^{-(T-t)\frac{|\lambda|^2}{2}}U(x), \quad \hat{\alpha}_i = \frac{\lambda_i}{\eta\sigma}.$$

We train with the forward process

$$X_{k+1} = X_k + \lambda\Delta t_k + \Delta W_k, \quad k = 0, \dots, N, \quad X_0 = x_0.$$

- (2) *One risky asset:  $n = 1$ .* A quasi-explicit solution is provided in [Zar01]:

$$u(t, x, v) = U(x)w(t, v), \quad \text{with } w(t, v) = \left\| \exp\left(-\frac{1}{2}\int_t^T R(\hat{V}_s^{t,v})ds\right) \right\|_{L^{1-\rho^2}}$$

where  $\hat{V}_s^{t,v}$  is the solution to the modified O.U. model

$$d\hat{V}_s = [\kappa(\theta - \hat{V}_s) - \rho\nu\lambda(\hat{V}_s)]ds + \nu dB_s, \quad s \geq t, \quad \hat{V}_t = v.$$

We test our algorithm with  $\lambda(v) = \lambda v$ ,  $\lambda > 0$ , for which we have an explicit solution:

$$w(t, v) = \exp\left(-\phi(t)\frac{v^2}{2} - \psi(t)v - \chi(t)\right), \quad (t, v) \in [0, T] \times \mathbb{R},$$

where  $(\phi, \psi, \chi)$  are solutions of the Riccati system of ODEs:

$$\begin{aligned} \dot{\phi} - 2\bar{\kappa}\phi - \nu^2(1 - \rho^2)\phi^2 + \lambda^2 &= 0, & \phi(T) &= 0, \\ \dot{\psi} - (\bar{\kappa} + \nu^2(1 - \rho^2)\phi)\psi + \kappa\theta\phi &= 0, & \psi(T) &= 0, \\ \dot{\chi} + \kappa\theta\psi - \frac{\nu^2}{2}(-\phi + (1 - \rho^2)\phi^2) &= 0, & \chi(T) &= 0, \end{aligned}$$

with  $\bar{\kappa} = \kappa + \rho\nu\lambda$ , and explicitly given by (see e.g. Appendix in [SZ99])

$$\begin{aligned}\phi(t) &= \lambda^2 \frac{\sinh(\hat{\kappa}(T-t))}{\hat{\kappa} \cosh(\hat{\kappa}(T-t)) + \bar{\kappa} \sinh(\hat{\kappa}(T-t))} \\ \psi(t) &= \lambda^2 \frac{\kappa\theta}{\hat{\kappa}} \frac{\cosh(\hat{\kappa}(T-t)) - 1}{\hat{\kappa} \cosh(\hat{\kappa}(T-t)) + \bar{\kappa} \sinh(\hat{\kappa}(T-t))} \\ \chi(t) &= \frac{1}{2(1-\rho^2)} \ln [\cosh(\hat{\kappa}(T-t)) + \frac{\bar{\kappa}}{\hat{\kappa}} \sinh(\hat{\kappa}(T-t))] - \frac{1}{2(1-\rho^2)} \bar{\kappa}(T-t) \\ &\quad - \lambda^2 \frac{(\kappa\theta)^2}{\hat{\kappa}^2} \left[ \frac{\sinh(\hat{\kappa}(T-t))}{\hat{\kappa} \cosh(\hat{\kappa}(T-t)) + \bar{\kappa} \sinh(\hat{\kappa}(T-t))} - (T-t) \right] \\ &\quad - \lambda^2 \frac{(\kappa\theta)^2 \bar{\kappa}}{\hat{\kappa}^3} \frac{\cosh(\hat{\kappa}(T-t)) - 1}{\hat{\kappa} \cosh(\hat{\kappa}(T-t)) + \bar{\kappa} \sinh(\hat{\kappa}(T-t))},\end{aligned}$$

with  $\hat{\kappa} = \sqrt{\kappa^2 + 2\rho\nu\lambda\kappa + \gamma^2\lambda^2}$ . We train with the forward process

$$\begin{aligned}\mathcal{X}_{k+1} &= \mathcal{X}_k + \lambda\theta\Delta t_k + \Delta W_k, \quad k = 0, \dots, N-1, \quad \mathcal{X}_0 = x_0, \\ V_{k+1} &= V_k + \nu\Delta B_k, \quad k = 0, \dots, N-1, \quad V_0 = \theta.\end{aligned}$$

(3) *No leverage effect*, i.e.,  $\rho_i = 0$ ,  $i = 1, \dots, n$ . In this case, there is a quasi-explicit solution given by

$$u(t, x, v) = U(x)w(t, v), \quad \text{with } w(t, v) = \mathbb{E} \left[ \exp \left( -\frac{1}{2} \int_t^T R(V_s^{t,v}) ds \right) \right], \quad (t, v) \in [0, T] \times \mathbb{R}^n, \quad (3.4)$$

where  $V^{t,v}$  is the solution to (3.2), starting from  $v$  at time  $t$ . We test our algorithm with  $\lambda_i(v) = \lambda_i v_i$ ,  $\lambda_i > 0$ ,  $i = 1, \dots, n$ ,  $v = (v_1, \dots, v_n)$ , for which we have an explicit solution given by

$$\begin{aligned}w(t, v) &= \exp \left( -\sum_{i=1}^n \left[ \phi_i(t) \frac{v_i^2}{2} + \psi_i(t) v_i + \chi_i(t) \right] \right), \quad (t, v) \in [0, T] \times \mathbb{R}^n, \\ \phi_i(t) &= \lambda_i^2 \frac{\sinh(\hat{\kappa}_i(T-t))}{\kappa_i \sinh(\hat{\kappa}_i(T-t)) + \hat{\kappa}_i \cosh(\hat{\kappa}_i(T-t))} \\ \psi_i(t) &= \lambda_i^2 \frac{\kappa_i \theta_i}{\hat{\kappa}_i} \frac{\cosh(\hat{\kappa}_i(T-t)) - 1}{\hat{\kappa}_i \cosh(\hat{\kappa}_i(T-t)) + \kappa_i \sinh(\hat{\kappa}_i(T-t))} \\ \chi_i(t) &= \frac{1}{2} \ln [\cosh(\hat{\kappa}_i(T-t)) + \frac{\kappa_i}{\hat{\kappa}_i} \sinh(\hat{\kappa}_i(T-t))] - \frac{1}{2} \kappa_i (T-t) \\ &\quad - \lambda_i^2 \frac{(\kappa_i \theta_i)^2}{\hat{\kappa}_i^2} \left[ \frac{\sinh(\hat{\kappa}_i(T-t))}{\hat{\kappa}_i \cosh(\hat{\kappa}_i(T-t)) + \kappa_i \sinh(\hat{\kappa}_i(T-t))} - (T-t) \right] \\ &\quad - \lambda_i^2 \frac{(\kappa_i \theta_i)^2 \kappa_i}{\hat{\kappa}_i^3} \frac{\cosh(\hat{\kappa}_i(T-t)) - 1}{\hat{\kappa}_i \cosh(\hat{\kappa}_i(T-t)) + \kappa_i \sinh(\hat{\kappa}_i(T-t))},\end{aligned}$$

with  $\hat{\kappa}_i = \sqrt{\kappa_i^2 + \nu_i^2 \lambda_i^2}$ . We train with the forward process

$$\begin{aligned}\mathcal{X}_{k+1} &= \mathcal{X}_k + \sum_{i=1}^n \lambda_i \theta_i \Delta t_k + \Delta W_k, \quad k = 0, \dots, N-1, \quad \mathcal{X}_0 = x_0, \\ V_{k+1}^i &= V_k^i + \nu_i \Delta B_k^i, \quad k = 0, \dots, N-1, \quad V_0^i = \theta_i,\end{aligned}$$

with  $\langle W, B^i \rangle_t = 0$ .

**Merton Problem.** We take  $\eta = 0.5$ ,  $\lambda = 0.6$ ,  $T = 1$ ,  $N = 120$ , and  $\sigma(v) = e^v$ . We plot the neural networks approximation of  $u$ ,  $D_x u$ ,  $D_x^2 u$ ,  $\alpha$  (in blue) together with their analytic values (in orange).

Averaged value	Standard deviation	Relative error (%)
-0.50510	0.00393	0.30

Figure 15: Estimate of  $u(0, x_0 = 1)$  in the Merton problem (3.3). Average and standard deviation observed over 10 independent runs are reported. The theoretical solution is -0.50662.



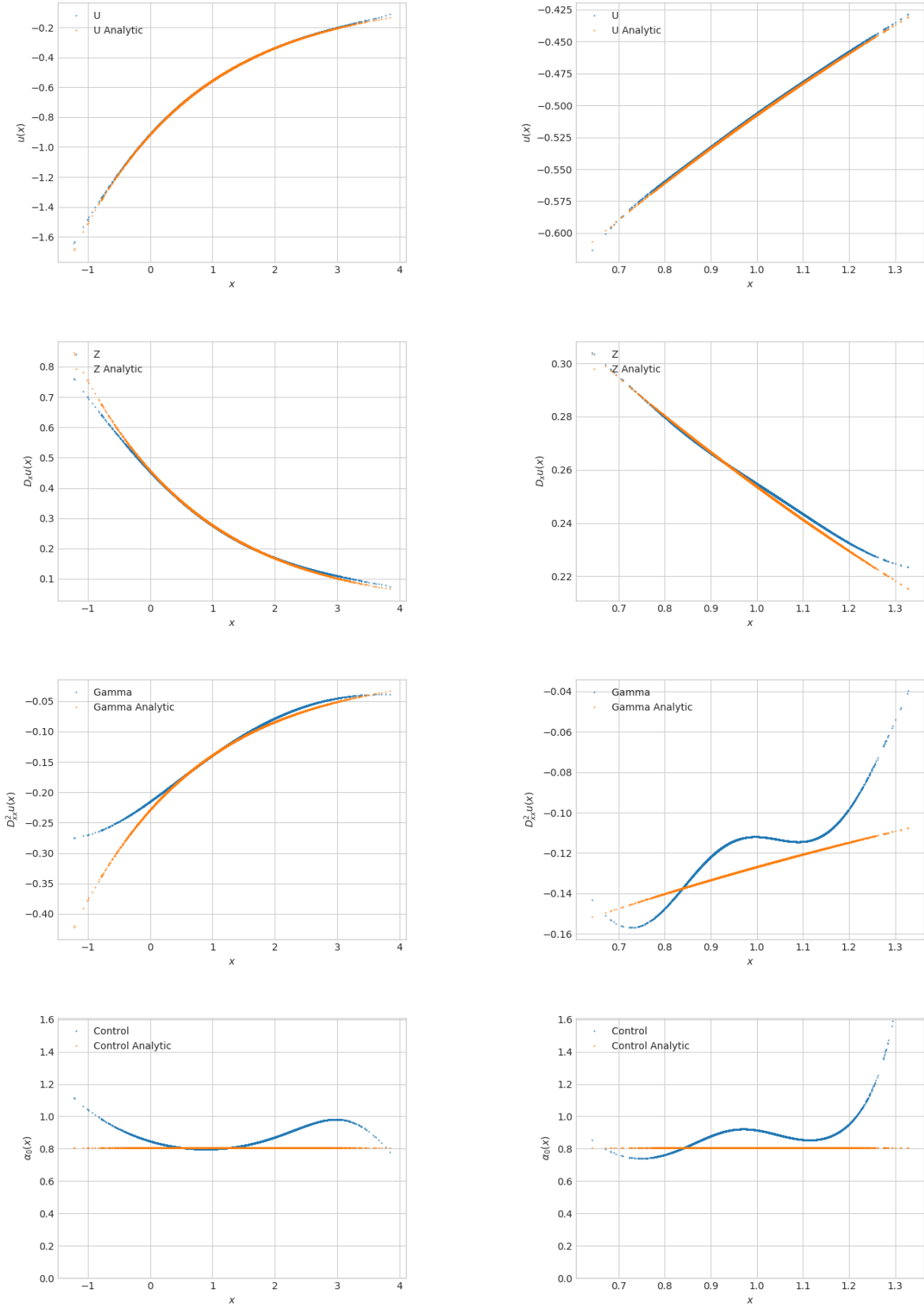


Figure 16: Estimates of  $u$ ,  $D_x u$ ,  $D_x^2 u$  and of the optimal control  $\alpha$  on the Merton problem (3.3). We take  $x_0 = 1$ , at the left  $t = 0.5042$ , and at the right  $t = 0.0084$ .

**One asset ( $n = 1$ ) in Scott volatility model.** We take  $\eta = 0.5$ ,  $\lambda = 1.5$ ,  $\theta = 0.4$ ,  $\nu = 0.4$ ,  $\kappa = 1$ ,  $\rho = -0.7$ . For all tests we choose  $T = 1$ ,  $N = 120$ , and  $\sigma(v) = e^v$ . We plot the error between the neural networks approximation of  $u$ ,  $D_x u$ ,  $D_x^2 u$  and their analytic values.

Averaged value	Standard deviation	Relative error (%)
-0.53327	0.00619	0.53

Figure 17: Estimate of  $u(0, x_0 = 1, \theta)$  on the One Asset problem with stochastic volatility ( $d = 2$ ). Average and standard deviation observed over 10 independent runs are reported. The exact solution is  $-0.53609477$ .

**No Leverage in Scott model.** In the case with one asset ( $n = 1$ ), we take  $\eta = 0.5$ ,  $\lambda = 1.5$ ,  $\theta = 0.4$ ,  $\nu = 0.2$ ,  $\kappa = 1$ . For all tests we choose  $T = 1$ ,  $N = 120$ , and  $\sigma(v) = e^v$ . We plot the error between the neural networks approximation of  $u$ ,  $D_x u$ ,  $D_x^2 u$  and their analytic values.

Averaged value	Standard deviation	Relative error (%)
-0.50160	0.00594	0.007

Figure 18: Estimate of  $u(0, x_0 = 1, \theta)$  on the No Leverage problem (3.4) with one asset ( $d = 2$ ). Average and standard deviation observed over 10 independent runs are reported. The exact solution is  $-0.501566$ .

In the case with four assets ( $n = 4$ ), we take  $\eta = 0.5$ ,  $\lambda = (1.5 \ 1.1 \ 2. \ 0.8)$ ,  $\theta = (0.1 \ 0.2 \ 0.3 \ 0.4)$ ,  $\nu = (0.2 \ 0.15 \ 0.25 \ 0.31)$ ,  $\kappa = (1. \ 0.8 \ 1.1 \ 1.3)$ .

Averaged value	Standard deviation	Relative error (%)
-0.45119	0.00507	2.13

Figure 19: Estimate of  $u(0, x_0 = 1, \theta)$  on the No Leverage problem (3.4) with four assets ( $d = 5$ ) and  $N = 120$ . Average and standard deviation observed over 10 independent runs are reported. The theoretical solution is  $-0.44176462$ .

In the case with seven assets we take  $\eta = 0.5$ ,  $\lambda = (1.5 \ 1.1 \ 2. \ 0.8 \ 0.5 \ 1.7 \ 0.9)$ ,  $\theta = (0.1 \ 0.2 \ 0.3 \ 0.4 \ 0.25 \ 0.15 \ 0.18)$ ,  $\nu = (0.2 \ 0.15 \ 0.25 \ 0.31 \ 0.4 \ 0.35 \ 0.22)$ ,  $\kappa = (1. \ 0.8 \ 1.1 \ 1.3 \ 0.95 \ 0.99 \ 1.02)$ .

Averaged value	Standard deviation	Relative error (%)
-0.40146	0.00819	1.65

Figure 20: Estimate of  $u(0, x_0 = 1, \theta)$  on the No Leverage problem with seven assets ( $d = 8$ ) and  $N = 120$ . Average and standard deviation observed over 10 independent runs are reported. The theoretical solution is  $-0.39493783$ .

In the case with nine assets ( $n = 9$ ), we take  $\eta = 0.5$ ,  $\lambda = (1.5 \ 1.1 \ 2. \ 0.8 \ 0.5 \ 1.7 \ 0.9 \ 1. \ 0.9)$ ,  $\theta = (0.1 \ 0.2 \ 0.3 \ 0.4 \ 0.25 \ 0.15 \ 0.18 \ 0.08 \ 0.91)$ ,  $\nu = (0.2 \ 0.15 \ 0.25 \ 0.31 \ 0.4 \ 0.35 \ 0.22 \ 0.4 \ 0.15)$ ,  $\kappa = (1. \ 0.8 \ 1.1 \ 1.3 \ 0.95 \ 0.99 \ 1.02 \ 1.06 \ 1.6)$ .

Averaged value	Standard deviation	Relative error (%)
-0.30150	0.03475	9.60

Figure 21: Estimate of  $u(0, x_0 = 1, \theta)$ , with 120 time steps on the No Leverage problem with 9 assets ( $d = 10$ ) and  $N = 120$ . Average and standard deviation observed over 10 independent runs are reported. The theoretical solution is  $-0.27509173$ .

Hamilton-Jacobi-Bellman equation from portfolio optimization is a typical example of full-nonlinearity in the second order derivative, and the above results show that our algorithm performs quite well up to dimension  $d = 8$ , but does not give accurate approximation in dimension  $d = 10$ . We conclude this paper with some comparison of our algorithm with the the global scheme of [BEJ19], called Deep 2BDSE. This scheme was implemented in the original paper only for small number of time steps (e.g.  $N = 30$ ), and so we tested this algorithm on two discretizations, respectively with  $N = 20$  and  $N = 120$  time steps, as shown in figure 22, where we plotted the learning curve of the loss function in terms of the number of gradient descent iterations. Even when decreasing the learning rate, we observe that it does not help to obtain the convergence of the scheme. However, the Deep 2BSDE method converges for small maturities, as illustrated in figure 23. The tests below concern the Merton problem but similar behavior happens on the other examples with stochastic volatilities.

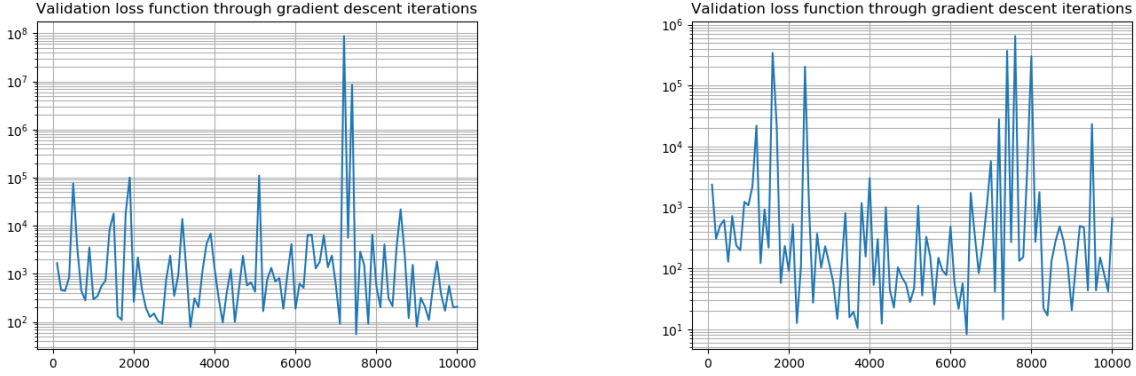


Figure 22: Learning curve in logarithmic scale for the scheme [BEJ19] on the Merton problem (3.3) with  $N = 20$  times steps on the left and  $N = 120$  time steps on the right. 10000 gradient descent iterations were conducted.

$N$	Averaged value	Standard deviation	Relative error (%)
5	-0.59490	0.03323	0.14
10	-0.61843	0.03097	3.81
20	-0.60780	0.03987	2.03

Figure 23: Estimate of  $u(0, x_0 = 1)$  in the Merton problem (3.3) with  $T = 0.1$  using [BEJ19]. Average and standard deviation observed over 10 independent runs are reported. The theoretical solution is  $Y_0 = -0.5957108$ .

$N$	Averaged value	Standard deviation	Relative error (%)
5	-0.02559	0.47267	108.59
10	0.18009	0.45100	39.54
20	0.16433	0.39681	44.83

Figure 24: Estimate of  $D_x u(0, x_0 = 1)$  in the Merton problem (3.3) with  $T = 0.1$  using [BEJ19]. Average and standard deviation observed over 10 independent runs are reported. The theoretical solution is  $Z_0 = 0.2978554$ .

## References

- [AA+18] A. Al-Aradi et al. “Solving Nonlinear and High-Dimensional Partial Differential Equations via Deep Learning”. In: *arXiv:1811.08782* (2018).
- [Aba+15] M. Abadi et al. *TensorFlow: Large-Scale Machine Learning on Heterogeneous Systems*. Software available from tensorflow.org. 2015. URL: <https://www.tensorflow.org/>.
- [Bec+19] C. Beck et al. “Deep splitting method for parabolic PDEs”. In: *arXiv:1907.03452* (2019).
- [BEJ19] C. Beck, W. E, and A. Jentzen. “Machine Learning Approximation Algorithms for High-Dimensional Fully Nonlinear Partial Differential Equations and Second-order Backward Stochastic Differential Equations”. In: *J. Nonlinear Sci.* 29.4 (2019), pp. 1563–1619.
- [Che+07] P. Cheridito et al. “Second-order backward stochastic differential equations and fully nonlinear parabolic PDEs”. In: *Communications on Pure and Applied Mathematics* 60.7 (2007), pp. 1081–1110.
- [CWNMW19] Quentin Chan-Wai-Nam, Joseph Mikael, and Xavier Warin. “Machine learning for semi linear PDEs”. In: *Journal of Scientific Computing* 79.3 (2019), pp. 1667–1712.
- [DLM19] J. Darbon, G. Langlois, and T. Meng. “Overcoming the curse of dimensionality for some Hamilton-Jacobi partial differential equations via neural network architectures”. In: *arXiv:1910.09045* (2019).
- [EHJ17] W. E, J. Han, and A. Jentzen. “Deep learning-based numerical methods for high-dimensional parabolic partial differential equations and backward stochastic differential equations”. In: *Communications in Mathematics and Statistics* 5.4 (2017), pp. 349–380.
- [FTW11] A. Fahim, N. Touzi, and X. Warin. “A probabilistic numerical method for fully nonlinear parabolic PDEs”. In: *The Annals of Applied Probability* (2011), pp. 1322–1364.

- [HE18] J. Han and A. Jentzen W. E. “Solving high-dimensional partial differential equations using deep learning”. In: *Proceedings of the National Academy of Sciences of the United States of America* 115.34 (2018), pp. 8505–8510.
- [HPW19] C. Huré, H. Pham, and X. Warin. “Deep backward schemes for high-dimensional nonlinear PDEs”. In: *arXiv:1902.01599, to appear in Mathematics of Computation* (2019).
- [Hut+18] M. Hutzenthaler et al. “Overcoming the curse of dimensionality in the numerical approximation of semilinear parabolic partial differential equations”. In: *arXiv:1807.01212* (2018).
- [KB14] D. P. Kingma and J. Ba. *Adam: A Method for Stochastic Optimization*. Published as a conference paper at the 3rd International Conference for Learning Representations, San Diego, 2015. 2014. URL: <http://arxiv.org/abs/1412.6980>.
- [Pha09] H. Pham. *Continuous-time Stochastic Control and Optimization with Financial Applications*. Vol. 61. SMAP. Springer, 2009.
- [Pin99] A. Pinkus. “Approximation theory of the MLP model in neural networks”. In: *Acta numerica* 8 (1999), pp. 143–195.
- [SS18] J. Sirignano and K. Spiliopoulos. “DGM: A deep learning algorithm for solving partial differential equations”. In: *Journal of Computational Physics* 375 (2018), pp. 1339–1364.
- [SZ99] R. Schöbel and J. Zhu. “Stochastic volatility with an Ornstein-Uhlenbeck process and extension”. In: *Review of Finance* 3.1 (1999), pp. 23–46.
- [Tan13] X. Tan. “A splitting method for fully nonlinear degenerate parabolic PDEs”. In: *Electronic Journal of Probability* 18 (2013).
- [VSS18] M. Sabate Vidales, D. Siska, and L. Szpruch. “Unbiased deep solvers for parametric PDEs”. In: *arXiv:1810.05094v2* (2018).
- [War18] X. Warin. “Monte Carlo for high-dimensional degenerated Semi Linear and Full Non Linear PDEs”. In: *arXiv:1805.05078* (2018).
- [Zar01] T. Zariphopoulou. “A solution approach to valuation with unhedgeable risks”. In: *Finance and Stochastics* 5 (2001), pp. 61–82.